J. Am. Soc. Mass Spectrom. (2017) 28:619–627
DOI: 10.1007/s13361-017-1605-3

FOCUS: EMERGING INVESTIGATORS: RESEARCH ARTICLE

Molecular Structures and Momentum Transfer Cross Sections: The Influence of the Analyte Charge Distribution

Meggie N. Young,[1] Christian Bleiholder[1,2]

[1]Department of Chemistry and Biochemistry, Florida State University, Tallahassee, FL 32306, USA
[2]Institute of Molecular Biophysics, Florida State University, Tallahassee, FL 32306, USA

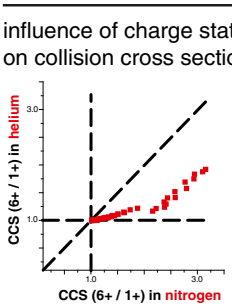

Abstract. Structure elucidation by ion mobility spectrometry-mass spectrometry methods is based on the comparison of an experimentally measured momentum transfer cross-section to cross-sections calculated for model structures. Thus, it is imperative that the calculated cross-section must be accurate. However, it is not fully understood how important it is to accurately model the charge distribution of an analyte ion when calculating momentum transfer cross-sections. Here, we calculate and compare momentum transfer cross-sections for carbon clusters that differ in mass, charge state, and mode of charge distribution, and vary temperature and polarizability of the buffer gas. Our data indicate that the detailed distribution of the ion charge density is intimately linked to the contribution of glancing collisions to the momentum transfer cross-section. The data suggest that analyte ions with molecular mass ~3 kDa or momentum transfer cross-section 400–500 Å^2 would be significantly influenced by the charge distribution in nitrogen buffer gas. Our data further suggest that accurate structure elucidation on the basis of IMS-MS data measured in nitrogen buffer gas must account for the molecular charge distribution even for systems as large as C_{960} (~12 kDa) when localized charges are present and/or measurements are conducted under cryogenic temperatures. Finally, our data underscore that accurate structure elucidation is unlikely if ion mobility data recorded in one buffer gas is converted into other buffer gases when electronic properties of the buffer gases differ.

Keywords: Ion mobility spectrometry, Mass spectrometry, Momentum transfer cross-section, Ion-neutral interaction potential

Received: 4 August 2016/Revised: 19 December 2016/Accepted: 20 December 2016/Published Online: 1 March 2017

Introduction

Ion mobility spectrometry-mass spectrometry (IMS-MS) has recently gained significant attention to elucidate conformations of proteins and their complexes [1–7]. Structure elucidation by IMS-MS comprises two independent processes: momentum transfer cross-sections of analyte ions are measured experimentally and, subsequently, computational approaches are used to extract the analyte structure from the measured cross-section [8, 9]. Details of the experimental measurement process have been described in detail elsewhere [10]. Here, we emphasize that the accuracy by which the absolute momentum transfer cross-section $\Omega(T)$ is determined experimentally is crucial: any error made in measuring the absolute value of the momentum transfer cross-section will be carried forward to the computational analysis and, thus, bias the elucidated structure. Once the momentum transfer cross-section has been experimentally determined, computational tools are used to extract the structure of the analyte ion [11–15]. In principle, the basic workflow is straightforward: expected momentum transfer cross-sections are predicted for theoretical model structures and compared with the experiment. In practice, however, this process is non-trivial, particularly for complex analyte ions such as proteins.

One major unknown here is how the molecular charge distribution influences the momentum transfer cross-section of the analyte ion. The distribution of charges within the analyte ion can influence its momentum transfer cross-section in two distinct ways. First, the charge distribution can influence the momentum transfer cross-section *indirectly* through promoting structural changes of the analyte ion. For example, proteins with higher charge states are more prone to unfolding

Electronic supplementary material The online version of this article (doi:10.1007/s13361-017-1605-3) contains supplementary material, which is available to authorized users.

Correspondence to: Christian Bleiholder; *e-mail:* cbleiholder@fsu.edu

prior to or during the IMS-MS experiment than proteins with a lower charge state [16–18]. Consequently, high charge states of proteins usually exhibit significantly larger cross-sections than lower charge states [16, 19–21]. Secondly, the charge distribution can also *directly* influence the momentum transfer cross-section of an analyte ion through modulating the ion–buffer gas interaction potential [11, 22, 23]. Such effects would be observed even in the absence of any structural changes prior to or during the IMS-MS experiment.

For small analyte ions, such direct effects of the charge distribution on the momentum transfer cross-section have been observed [24–28]. Early studies conducted by Jarrold and co-workers [23] and Bowers et al. [28] demonstrated that cross-sections of carbon clusters measured in helium buffer gas depend on the charge state. One more recent example is a report by von Helden and co-workers on an IR study of mobility selected protomers of benzocaine [26]. Their results indicate that momentum transfer cross-sections of O- and N-protonated isomers of benzocaine can differ by ~10% in nitrogen buffer gas due to charge localization in the N-protonated "protomer." Notably, their study indicated that such charge localization effects depend on the polarizability of the buffer gas. More recently, Sobott and co-workers reported on the influence of the molecular charge distribution on the momentum transfer cross-section for several small molecules in nitrogen buffer gas [27]. Their data support the view that the molecular charge distribution can significantly influence the momentum transfer cross-section of small molecules in polarizable buffer gases. These studies are consistent with results reported from Hill and co-workers on momentum transfer cross-sections of para-halogenated anilines in helium, argon, nitrogen, and carbon dioxide buffer gases [25]. They found that the momentum transfer cross-sections correlate strongly linearly with the polarizability of the buffer gas. Intriguingly, their data reveal that in helium buffer gas para-iodoaniline is ~37% larger in momentum transfer cross-section than para-fluoroaniline, whereas in carbon dioxide para-iodoaniline is ~8% smaller in momentum transfer cross-section than para-fluoroaniline. Also, this observation was traced back to differences in electronic properties of the analyte ion and neutral gas particles, respectively.

For analyte ions as large and complex as proteins, the situation is not as clearly understood. When proteins are analyzed under native conditions, momentum transfer cross-sections of low charge states are typically consistent with the native protein structure [16, 19–21, 29]. By contrast, cross-sections for high charge states can be twice as large as expected for native protein structures. These large cross-sections observed for high charge states of proteins can be rationalized by charge state-dependent unfolding of the protein ion in the gas phase [17]. That is, by presuming that the charge distribution influences the momentum transfer cross-section indirectly through charge-state dependent structural dynamics of proteins in the IMS-MS experiment [18]. Such charge-state-dependent structural dynamics were recently described in detail by Bush and co-workers [30] for ubiquitin ions by cation to anion proton transfer reactions (CAPTR). However, the experimental data show that momentum transfer cross-sections also increase for low charge states of protein ions [19, 21, 29, 31, 32]. As one specific example, Bowers and co-workers reported that momentum transfer cross-sections of native-like ubiquitin for charge states +7 and +8 are ~3% and ~5% larger than charge state +6 in helium [31]. In nitrogen buffer gas, charge states +7 and +8 are ~6% and ~8% larger than charge state +6 [31, 32]. Similar observations were made by Barran and co-workers [21] for momentum transfer cross-sections of several proteins measured in neon, argon, and nitrogen buffer gases. Do these small increases in momentum transfer cross-section for low protein charge states arise from changes in the ion-neutral interaction potential? Or are they due to minor structural changes due to protein dynamics in the gas phase?

The discussion above illustrates that it is poorly understood how strongly the molecular charge distribution would affect the momentum transfer cross-section in the absence of structural dynamics. Here, we seek to identify in more general terms under what circumstances the charge distribution can be expected to directly influence the momentum transfer cross-section of an analyte ion. To this end, we use carbon clusters that differ in molecular mass as model systems and calculate their expected momentum transfer cross-sections for nitrogen and helium buffer gases, different temperatures, as a function of increasing charge state, and for different charge distributions.

Computational Details

We chose carbon clusters comprising 24, 60, 180, 240, 500, and 960 carbon atoms as model systems for the following reasons. First, the carbon–helium interaction parameters of the trajectory method were thoroughly parameterized to experimental momentum transfer cross-sections for Buckminster-fullerene (C_{60}) [11], and the trajectory method reproduces the experimentally determined temperature dependency of the C_{60} momentum transfer cross-section in the range of 80 to 500 K [15]. It can thus be expected that momentum transfer cross-sections calculated by the trajectory method for these systems are accurate. Additionally, these systems are highly symmetric and comprise only one type of atoms, which reduces complexity in the charge distribution as well as in the analysis of our computational data. Moreover, the molecular mass and momentum transfer cross-sections of these systems range from those typical for small organic molecules (300 Da and ~100 $Å^2$ in helium buffer gas) to small proteins (12 kDa and ~1000 $Å^2$ in helium buffer gas). The total charge on these systems was varied from +1 to +6 to simulate multiply charged systems that are common to electrospray ionization. We used two distinct schemes to assign atomic point charges, which we termed "localized" and "dispersed." By dispersed charge distribution we mean

that the total charge of the analyte was uniformly distributed among all atoms in the molecule. By localized charge distribution we mean that integer charges were distributed among select atoms in the molecule. There are many ways to distribute integer charges in a polyatomic molecule. We distributed these integer charges such that Columbic repulsion between the charges was minimized (e.g., +2 in straight line, +4 similar to a tetrahedron, or +6 similar to an octahedron). These two modes of charge distribution were motivated to assess qualitatively how strongly the momentum transfer cross-section of an analyte ion is affected when charges are sequestered at specific locations in the analyte ion, such as by salt adducts or strongly basic residues in a peptide or protein ion. Specific charge distributions by particular computational procedures were not calculated so that our discussion is not biased to a specific, artificial definition of atomic charges (see below). All momentum transfer cross-sections were calculated for temperatures ranging from 80 to 700 K with the trajectory method as implemented in the MOBCAL-He [11] and MOBCAL-N_2 [22, 33] programs. All calculated cross-sections can be found in Table S1 in the Supporting Information.

Results and Discussion

Background

Many algorithms are available to calculate momentum transfer cross-sections for theoretical model structures but only the scattering on electron density isosurfaces (SEDI) [14, 34], local collision probability approximation (LCPA) [35], and trajectory methods [11, 22, 33] are capable to explicitly consider details of the ion's charge distribution. From a physical perspective, the trajectory method is conceptually the most rigorous approach because it simulates the physical collision process within the limits of classic mechanics. The trajectory method calculates the momentum transfer cross-section $\Omega(T)$ from millions of ion-neutral collisions with deflection angles θ [36] according to

$$\Omega(T) = 2\pi \int_0^{\infty} d\varepsilon \int_0^{\pi} d\theta\, f(\varepsilon, T)(1-\cos\theta)\sigma(\varepsilon,\theta)\sin\theta \qquad (1)$$

Here, $f(\varepsilon, T)$ is the Boltzmann distribution of the kinetic energy ε for an analyte ion–buffer gas system at temperature T, $\sigma(\varepsilon,\theta)$ is the differential collision cross-section, and the term $(1-\cos\theta)$ corresponds to the fraction of momentum transferred via a collision with deflection angle θ and can take on values between 0 ($\theta = 0$) and 2 ($\theta = \pi$, head-on collision). The individual deflection angles θ are calculated by solving Newton's equations of motion on an ion-neutral interaction potential $U(\boldsymbol{r})$. This ion-neutral interaction potential $U(\boldsymbol{r})$ is estimated in the MOBCAL implementation [11, 22, 33] as a sum of two-body interaction terms according to:

$$U(\boldsymbol{r}) = \sum_{i=1}^{atoms} E_i \left[\left(\frac{r_{min,i}}{|\boldsymbol{r} - \boldsymbol{R}_i|} \right)^{12} - \left(\frac{r_{min,i}}{|\boldsymbol{r} - \boldsymbol{R}_i|} \right)^{6} \right] + V(\boldsymbol{r}) + \Phi(\boldsymbol{r}) \qquad (2)$$

Here, $\boldsymbol{r}$ is the position of the buffer gas particle relative to the center-of-mass of the analyte ion, E_i and $r_{min,i}$ are the Lennard-Jones parameters, $\boldsymbol{R}_i$ the centers of the atoms, and $V(\boldsymbol{r})$ and $\Phi(\boldsymbol{r})$ are the induction and electrostatic components to $U(\boldsymbol{r})$ arising from electric multipole moments and polarizabilities of the ion and buffer gas particles. For helium, Jarrold and coworkers [11] ignore $\Phi(\boldsymbol{r})$ and express the charge-induced interaction $V(\boldsymbol{r})$ according to

$$V(\boldsymbol{r}) = -\frac{\alpha}{2} \left[\left(\sum_i^{atoms} \frac{q_i x_i}{|\boldsymbol{r} - \boldsymbol{R}_i|^3} \right)^2 + \left(\sum_i^{atoms} \frac{q_i y_i}{|\boldsymbol{r} - \boldsymbol{R}_i|^3} \right)^2 + \left(\sum_i^{atoms} \frac{q_i z_i}{|\boldsymbol{r} - \boldsymbol{R}_i|^3} \right)^2 \right] \qquad (3)$$

Here, α is the polarizability of the neutral gas, q_i the atomic partial charge, and x_i, y_i, z_i are defined by the relative position of the atoms with respect to the buffer gas particle according to

$$\begin{pmatrix} x_i \\ y_i \\ z_i \end{pmatrix} = \boldsymbol{R}_i - \boldsymbol{r} \qquad (4)$$

These expressions are then used to calculate a large number of deflection angles θ to predict the momentum transfer cross-section $\Omega(T)$ according to Equation 1. For nitrogen, Kim et al. take interactions between the ion charge distribution and the electrical quadrupole moment of nitrogen into account when calculating $\Phi(\boldsymbol{r})$ [22].

We emphasize that the functional form used in the trajectory method [11, 22, 33] to express the ion-neutral interaction potential is by no means rigorous. A thorough discussion of the ion-neutral interaction potential will be given elsewhere; here, we stress two issues. First, the ion-neutral interaction potential is rigorously expressed only on the basis of symmetry-adapted perturbation theory (SAPT) as a sum of electrostatic, dispersion, induction, and exchange interactions [37, 38]. Second, atomic charges are not a quantum-mechanical observable. Hence, representing the molecular charge distribution by a distribution of atomic point charges is not straightforward. In fact, there are many distinct definitions of how a molecular charge distribution can be separated into atomic components, including Mulliken [39], Hirshfeld [40], or natural atomic orbital [41] population analyses, Bader's atom-in-molecule analysis [42], or electrostatic potential-derived [43] charges. Absolute values of atomic point charges can depend drastically on the specific definition used for their calculation,

but also on the level of theory, basis set, and even the molecular conformation. Moreover, Chirlian and Francl [44] showed that atoms in similar chemical environments can be given different fitted charges by the electrostatic potential scheme [43], which has recently become popular as input for MOBCAL cross-section calculations [26, 27, 45]. Thus, we refrain from explicitly calculating atomic point charges by a specific scheme in order to not bias our discussion on a specific definition of point charges or level of theory. Instead, our focus will be to discuss—in more general terms—how strongly and how mechanistically the charge distribution influences the momentum transfer cross-section of an ion.

Influence of Ion Charge State on the Momentum Transfer Cross-Section as a Function of the Buffer Gas Polarizability

Bowers et al. [28] and Jarrold and co-workers [23] studied mobilities of C_{60} in helium buffer gas for charge states +1 to +4. The experiments show that the momentum transfer cross-section of C_{60} increases from ~130 $Å^2$ (+1 charge state) to ~150$Å^2$ (+4 charge state). Our calculations for C_{60} agree well with these experimental values (see Figure S2, Supporting Information).

In Figure 1 we correlate the ratio $\Omega^{(+6)}/\Omega^{(+1)}$ of momentum transfer cross-sections calculated for charge states +6 and +1 in helium to those in nitrogen buffer gas for all model systems and temperatures in the range from 80 to 700 K. Charges are uniformly distributed among all atoms of the ions. Two observations can be made in the Figure. First, the ratio $\Omega^{(+6)}/\Omega^{(+1)}$ is always greater than one for all buffer gases, model systems, and temperatures. This observation shows that the momentum transfer cross-section increases with increasing charge of the analyte ion. We rationalize this observation by noting that an increase in charge will increase the magnitude of the induction interaction term $V(\boldsymbol{r})$ (see Equation 3). Consequently, the ion-neutral interaction potential is deepened and, thus, the range of the ion-neutral interaction potential is extended as the charge is increased. Due to this extended range of the interaction potential, glancing collisions can be expected to increase in significance when the ion charge is increased, which increases the momentum transfer cross-section of the analyte. It is important to note that the induction interaction is independent of the sign of the charge as the charge enters Equation 3 quadratically. Hence, the discussion here made on the basis of positively charged ions pertains equally to ions with negative charge. Further, our data show that the calculated ratio $\Omega^{(+6)}/\Omega^{(+1)}$ is always larger for nitrogen buffer gas than it is for helium buffer gas. As discussed [31], this observation can be rationalized by the larger polarizability volume of nitrogen ($\alpha' = 1.74$ $Å^3$) [36] than that of helium ($\alpha' = 0.205$ $Å^3$) [36, 46]. The point here is that the magnitude of the induction interaction term $V(\boldsymbol{r})$ in Equation 3 is proportional to the polarizability volume of the neutral buffer gas particles. Hence, the range of the ion–nitrogen interaction potential is more significantly extended by the ion's charge than the ion–helium interaction potential. We extrapolate that momentum transfer cross-sections measured in buffer gases with significant electric multipole moments, such as carbon monoxide or dioxide, will experience an even greater influence of the molecular charge distribution. The reason for this is that the electrostatic component of the ion neutral interaction potential is typically stronger and longer in range than the induction and dispersion interactions [37, 38].

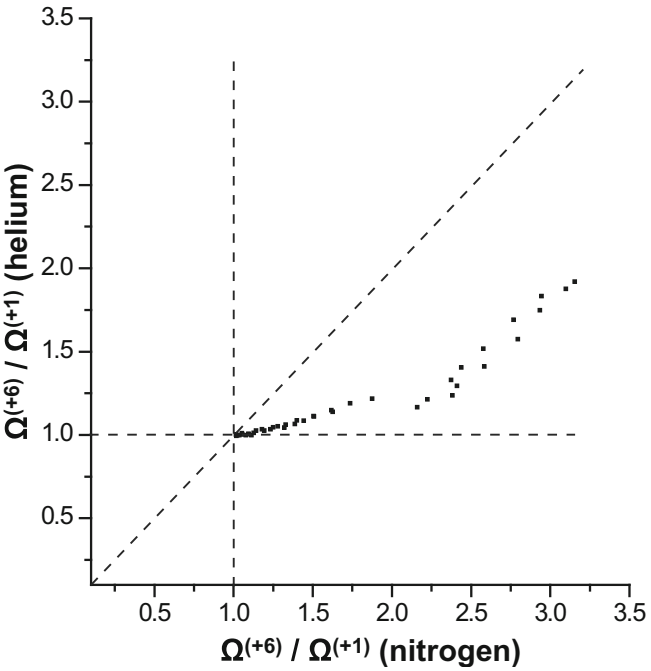

Figure 1. Correlation between ratios of momentum transfer cross-sections $\Omega^{(+6)}/\Omega^{(+1)}$ calculated for charge states +6 and +1 in helium to those in nitrogen buffer gas for all model systems and temperatures in the range from 80 to 700 K. The data show that the ratio $\Omega^{(+6)}/\Omega^{(+1)}$ is always greater than one, for all buffer gases, model systems, and temperatures. Further, the data reveal that the calculated ratio $\Omega^{(+6)}/\Omega^{(+1)}$ is always larger for nitrogen buffer gas than it is for helium buffer gas

Influence of Ion Charge State on the Momentum Transfer Cross-Section as a Function of Temperature

Figure 2 shows momentum transfer cross-sections predicted for fullerene C_{60} in helium and nitrogen buffer gases in the temperature range from 80 to 700 K for total charges +1 and +4 (uniformly distributed among all atoms). For both buffer gases and charge states, we note that momentum transfer cross-sections increase with decreasing temperature. Such a "temperature effect" is expected from previous studies and has been rationalized by the increasing contribution of glancing collisions to the cross-sections with decreasing temperature [11, 12, 31]. Also in line with a previous report [31] is the observation that this temperature effect is more pronounced for

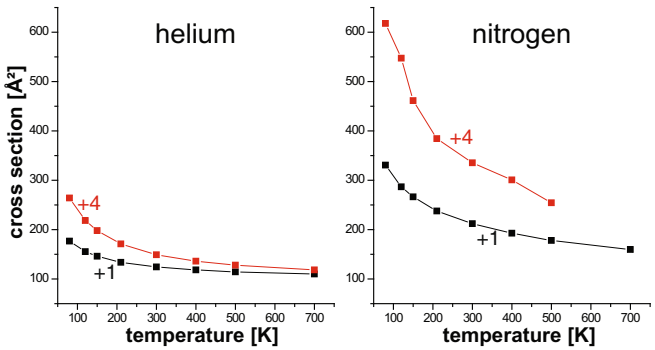

Figure 2. Momentum transfer cross-sections predicted for fullerene C_{60} in the temperature range from 80 to 700 K for total charges +1 and +4 for helium and nitrogen buffer gas. The data show that the momentum transfer cross-section increases with increasing ion charge state, buffer gas polarizability, and with decreasing temperature of the buffer gas

the more polarizable buffer gas nitrogen than it is for helium. This observation underscores that glancing collisions take on a more significant role for the more polarizable buffer gas nitrogen because the range of the ion–nitrogen interaction potential is longer reaching. Additionally, the data show that the increase in momentum transfer cross-section when the charge is increased from +1 to +4 is more pronounced at the lower temperature regime than it is at higher temperature. This observation indicates that the temperature- and charge-effects are coupled to each other. Moreover, the data show that this coupling of the temperature- and charge-effects is more pronounced for nitrogen than for helium buffer gas: the difference in momentum transfer cross-section between the +1 and +4 charge states is larger at 80 K (e.g., 87 Å^2 and 287 Å^2 for helium and nitrogen buffer gas, respectively) than at 500 K (e.g., 14 Å^2 and 76 Å^2 for helium and nitrogen buffer gas, respectively). In sum, we note that the significance of glancing collisions increases with (1) increase in ion charge, (2) increase of buffer gas polarizability, and (3) decrease in temperature. Hence, our data indicate that the molecular charge distribution must be accurately modeled if analyte structures are elucidated from IMS-MS data recorded at cryogenic temperatures, in particular in polarizable buffer gases.

Influence of Ion Charge State on the Momentum Transfer Cross-Section as a Function of Ion Mass

The previous section showed that the charge of the analyte ion significantly increases the momentum transfer cross-section of an ion by extending the range of the ion neutral interaction potential. It is known that the influence of the ion neutral interaction potential on the momentum transfer cross-section becomes increasingly negligible as the analyte approaches bulk matter [31, 47]. Hence, it is expected that the molecular charge distribution of an analyte ion influences the momentum transfer cross-section successively less as the analyte ion increases in molecular mass.

Figure 3 plots the calculated momentum transfer cross-sections for charge states +1, +2, +4, and +6 in helium and nitrogen buffer gas as a function of the molecular mass for model compounds C_{24}, C_{60}, C_{240}, C_{500}, and C_{960}. The total charges were equally distributed among all atoms. For brevity, we restrict the discussion here to 300 K but corresponding data for 120 K and 500 K are found in Figure S1 (see Supporting Information). In line with previous reports [48], the calculations show that, overall, the momentum transfer cross-sections increase with mass of the analyte ion. Further, we find that the charge of the ion increasingly influences the momentum transfer cross-section with decreasing mass of the ion: the calculated momentum transfer cross-section of C_{60} in nitrogen buffer gas increases by 16%, 58%, and 158% when the charge state is increased from +1 to +2, +4, and +6, respectively. For C_{960}, the influence of the charge state is much less pronounced; here, we find that increasing the charge state from +1 to +6 increases the momentum transfer cross-sections by only ~4%. These data support the previously made notion [31, 47] that the attractive well of the ion neutral interaction potential influences the momentum transfer process increasingly less as analyte ions increase in molecular mass. In line with our discussion above and a previous study [31], the influence of the ion charge on the momentum transfer cross-section in the less polarizable buffer gas helium is smaller: the calculated momentum transfer cross-section of C_{60} increases by 4%, 20%, and 52% when the charge state is increased from +1 to +2, +4, and +6, respectively, and essentially no effect is observed for C_{960}.

Our temperature-dependent data (see Figure S1 in the Supporting Information) indicate that the influence of the charge distribution on the momentum transfer cross-section increases significantly as the temperature is decreased and vice versa. This trend is expected from previous reports [11, 12, 31] and our discussion above because glancing collisions and the influence of the long-range of the ion neutral interaction potential contribute to the momentum transfer cross-section, especially at lower temperatures. Indeed, at 120 K, even the momentum transfer cross-section for C_{960} is calculated to increase by 11% when the charge is increased from +1 to +6 in nitrogen. This observation is important because it underscores that the charge state must be accurately modelled if IMS-MS data measured at cryogenic temperatures are used for structure elucidation, especially when the measurements are conducted in polarizable buffer gases.

Influence of Ion Charge State on the Momentum Transfer Cross-Section as a Function of the Mode of Charge Distribution

The previous sections showed that the total charge of the analyte ion can significantly influence the ion neutral interaction potential. In the calculations discussed above, the total charge was uniformly distributed among all atoms of the ion. In reality, however, atomic partial charges are not uniform but, instead, reflect the electron density. For large and complex systems, such as peptides or proteins, it is known that charges can be largely localized to specific functional groups, such as the highly basic guanidine or amino groups of arginine and

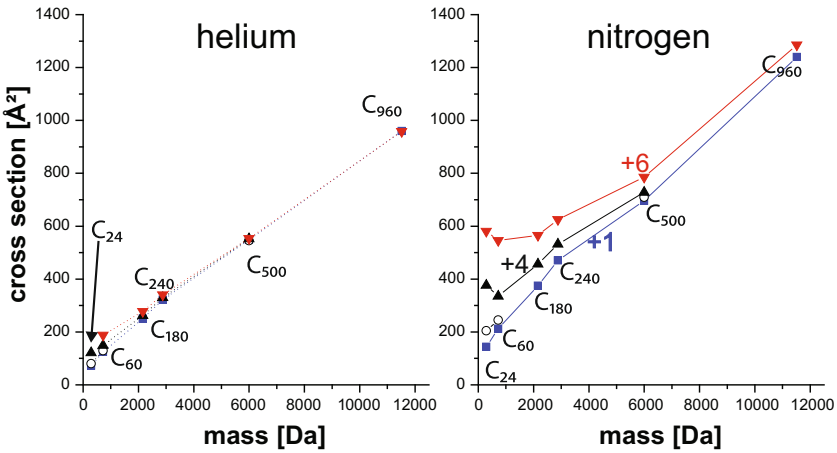

Figure 3. Calculated momentum transfer cross-sections for charge states +1 (blue squares), +2 (open circles), +4 (black triangles), and +6 (red inverse triangles) in helium and nitrogen buffer gas as a function of the ion mass for C_{24}, C_{60}, C_{180}, C_{240}, C_{500}, and C_{960}. The influence of the charge distribution on the momentum transfer cross-section decreases with increasing mass of the ion

lysine residues [49, 50], respectively. Thus, here we investigate how strongly the momentum transfer cross-section changes when the total charge is distributed in integer units instead of uniformly "smeared" among the atoms in the ion.

Figure 4 shows the ratio $\Omega_{loc}/\Omega_{disp}$ of momentum transfer cross-sections calculated with localized and dispersed charges for C_{60}, C_{240}, and C_{960} at 120 and 300 K for helium and nitrogen buffer gases and charge states +1 and +6. The data show that momentum transfer cross-sections calculated with a localized charge distribution are typically greater than momentum transfer cross-sections calculated from a uniformly dispersed charge distribution. We note only two exceptions from this trend, both for singly charged C_{960} at 300 K where the charge distribution has a fairly negligible effect on the momentum transfer cross-section ($\Omega_{loc}/\Omega_{disp}$~0.999 in both cases). Thus, overall, the data show that the momentum transfer cross-section of an analyte ion increases with charge localization. We observe the strongest effect for C_{60} in nitrogen buffer gas at 120 K (i.e., for a system with low molecular mass at low temperature in a polarizable buffer gas). Here, dispersing a single charge equally over the entire molecule reduces the momentum transfer cross-section from 300 to 287 Å^2 (i.e., by ~5%). Dispersing a total charge of 6+ reduces the momentum transfer cross-section of C_{60} from 975 to 904 Å^2 (i.e., by ~8%). The influence of the charge distribution decreases slightly as the mass of the analyte ion increases; however, the change in momentum transfer cross-section is substantial even for the largest molecules considered here. For instance, distribution of six charges for C_{240} and for C_{960} in nitrogen buffer gas at 300 K reduce the cross-sections by ~7% and ~3%, respectively. The ratio $\Omega_{loc}/\Omega_{disp}$ of C_{240}^{6+} is larger than that of C_{60}^{6+}, an apparent deviation from the trend. The cause for this deviation is not entirely obvious to us. However, we note that an analyte ion can only accommodate a certain number of localized, fully separated charges. We speculate that the six charges in C_{60}^{6+} are no longer truly "localized" while they still are localized in C_{240}^{6+}, resulting in a stronger charge effect for C_{240}^{6+}. Further, we point out that the effect of the charge distribution on the momentum transfer cross-section arises through modulation of the ion neutral interaction potential that determines the collision process. Hence, it is expected that the magnitude of the charge-effects discussed here will depend also on the geometry of the analyte ion. Indeed, Shvartsburg et al. [23] found that localized charges result in smaller cross-sections than distributed charges for linear carbon chains.

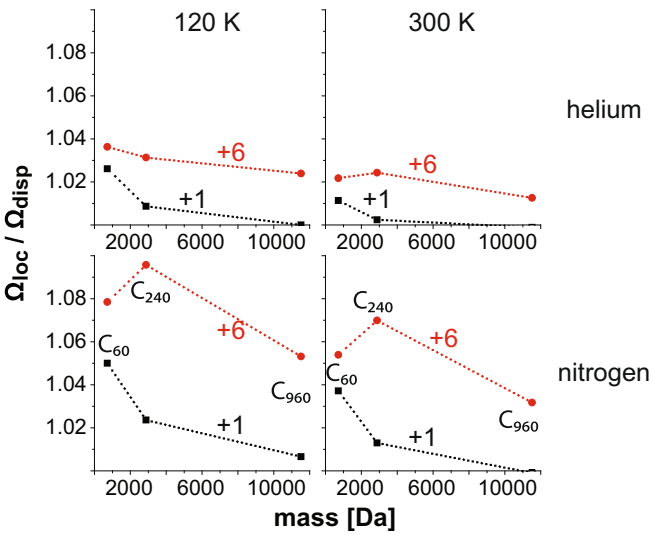

Figure 4. Ratio $\Omega_{loc}/\Omega_{disp}$ of momentum transfer cross-sections calculated with localized and distributed charges for C_{60}, C_{240}, and C_{960} at 120 and 300 K for helium and nitrogen buffer gases and charge states +1 and +6. Momentum transfer cross-sections calculated from a localized charge distribution are greater than those calculated from a dispersed charge distribution

However, overall, we observe that the significance of this "charge localization" effect increases with decreasing molecular mass, decreasing temperature, increasing buffer gas polarizability, and increasing total charge. These findings suggest that the detailed charge distribution of the analyte can be expected to significantly influence the momentum transfer cross-section. This influence is markedly apparent for multiply charged analytes when measured in polarizable buffer gas at lower temperatures. Although this effect is particularly pronounced for small molecular mass ions, our data suggest that analyte ions similar in mass to C_{960} can also be influenced by the specific charge distribution within the ion. Hence, the detailed distribution of the charge density can be expected to influence the momentum transfer cross-section also for protein systems such as ubiquitin (~8 kDa) or cytochrome *c* (~12 kDa). We emphasize that extra protons in a peptide or protein can be sequestered [49] to specific functional groups with high gas-phase basicity [50], such as the ring of histidine residues, or the guanidine and amino groups of arginine or lysine residues, respectively. Further, we note that also negatively charged residues are present in (multiply) protonated protein ions, even if the total charge state is positive. Since the magnitude of the induction interaction $V(\boldsymbol{r})$ is independent of the sign of charge, except for screening of charges of opposite sign, these localized positive and negative charges would jointly increase the magnitude of the induction interaction between the ion and the neutral buffer gas particles. Consequently, regions of both negative and positive charge can be expected to act largely cooperatively to deepen the ion neutral interaction potential and increase the momentum transfer cross-section of the analyte ion.

Bush and co-workers measured inverse mobilities, $1/K_0$, of peptides, denatured and native-like proteins, as well as singly charged sodium formate cluster ions in helium and nitrogen buffer gases [51]. They found that the correlation between $1/K_0$ measured in helium and nitrogen found for the biomolecules differs strongly from the relationship observed for the sodium formate cluster ions. Specifically, the inverse mobilities $1/K_0$ measured in nitrogen buffer gas for sodium formate cluster ions were larger than what would be expected from the inverse mobilities $1/K_0$ measured in helium based on the correlation established for the biomolecules. We note that singly charged sodium formate cluster ions comprise a number of negatively and positively charged ions, regardless of the overall charge state of +1. Hence, the charge distribution of these cluster ions differs strikingly from that of a singly charged molecular ion of similar size, such as a peptide. In the context of our discussion above, it can be extrapolated that the high density of negative and positive charges present in sodium formate cluster ions increases the magnitude of electrostatic and induction contributions to the ion neutral interaction potential over what would be observed for a molecular ion. Hence, as the momentum transfer cross-section in nitrogen buffer gas is much more susceptible to these charge-related effects, we would expect that the momentum transfer cross-section of these singly charged sodium formate cluster ions measured in nitrogen is larger than what would be expected on the basis of the biomolecule relationship.

Summary and Conclusion

We systematically investigated the influence of the ion charge distribution on the momentum transfer cross-section of an analyte ion in the absence of any structural dynamics. To this end, we calculated momentum transfer cross-sections for carbon cluster model systems and assessed how they change when varying temperature and polarizability of the buffer gas as well as mass, total charge, and charge distribution of the ion. Overall, our data indicate that the detailed distribution of the ion charge density is intimately linked to the contribution of glancing collisions to the momentum transfer cross-sections. Specifically, we find that the significance of the ion charge distribution increases with ion charge, buffer gas polarizability, and charge localization. Conversely, the significance of the ion charge distribution decreases as the buffer gas temperature and mass of the analyte ion increase. Our data indicate that computed momentum transfer cross-sections of multiply charged C_{240} in nitrogen buffer gas at 300 K depends significantly on the details of the charge distribution. It can be expected that analyte ions similar or smaller in mass (~3 kDa) or momentum transfer cross-section (400–500 $Å^2$) would also be significantly influenced by the charge distribution. Our data further indicate that accurate structure elucidation on the basis of IMS-MS data measured in nitrogen buffer gas must account for the molecular charge distribution even for systems as large as C_{960} (~12 kDa). Finally, our data underscore that accurate structure elucidation is unlikely if ion mobility data recorded in one buffer gas is converted into other buffer gases when the electronic properties of the buffer gases differ.

Supporting Information

Calculated momentum transfer cross-sections for carbon clusters C_{24}, C_{60}, C_{180}, C_{240}, C_{500}, and C_{960} for helium and nitrogen buffer gases, various charge states, localized and dispersed charge modes. Plots of the calculated cross-sections of fullerenes in He and N_2 buffer gas versus molecular mass showing gas polarizability-dependence and temperature dependence.

Acknowledgments

The authors acknowledge financial support from The Florida State University. The authors thank Martin Jarrold and Matthew Bush for making the helium and nitrogen implementations of the MOBCAL program available.

References

1. Ruotolo, B.T., Giles, K., Campuzano, I., Sandercock, A.M., Bateman, R.H., Robinson, C.V.: Evidence for macromolecular protein rings in the absence of bulk water. Science **310**, 1658–1661 (2005)
2. Bernstein, S.L., Dupuis, N.F., Lazo, N.D., Wyttenbach, T., Condron, M.M., Bitan, G., Teplow, D.B., Shea, J.-E., Ruotolo, B.T., Robinson, C.V., Bowers, M.T.: Amyloid-β protein oligomerization and the importance of tetramers and dodecamers in the aetiology of Alzheimer's disease. Nat. Chem. **1**, 326–331 (2009)
3. Bleiholder, C., Dupuis, N.F., Wyttenbach, T., Bowers, M.T.: Ion mobility-mass spectrometry reveals a conformational conversion from random assembly to β-sheet in amyloid fibril formation. Nat. Chem. **3**, 172–177 (2011)
4. Bleiholder, C., Do, T.D., Wu, C., Economou, N.J., Bernstein, S.S., Buratto, S.K., Shea, J.-E., Bowers, M.T.: Ion mobility spectrometry reveals the mechanism of amyloid formation of Aβ(25–35) and its modulation by inhibitors at the molecular level: epigallocatechin gallate and *scyllo*-inositol. J. Am. Chem. Soc. **135**, 16926–16937 (2013)
5. Young, L.M., Saunders, J.C., Mahood, R.A., Revill, C.H., Foster, R.J., Tu, L.-H., Raleigh, D.P., Radford, S.E., Ashcroft, A.E.: Screening and classifying small-molecule inhibitors of amyloid formation using ion mobility spectrometry-mass spectrometry. Nat. Chem. **7**, 73–81 (2014)
6. Alexander, C.G., Jürgens, M.C., Shepherd, D.A., Freund, S.M., Ashcroft, A.E., Ferguson, N.: Thermodynamic origins of protein folding, allostery, and capsid formation in the human hepatitis B virus core protein. Proc. Natl. Acad. Sci. **110**, E2782–E2791 (2013)
7. Harvey, S.R., MacPhee, C.E., Volkman, B.F., Barran, P.E.: The association and aggregation of the metamorphic chemokine lymphotactin with fondaparinux: from nm molecular complexes to μm molecular assemblies. Chem. Commun. **52**, 394–397 (2016)
8. Dupuis, N.F., Wu, C., Shea, J.-E., Bowers, M.T.: Human Islet amyloid polypeptide monomers form ordered β-hairpins: a possible direct amyloidogenic precursor. J. Am. Chem. Soc. **131**, 18283–18292 (2009)
9. Fernandez-Lima, F.A., Wei, H., Gao, Y.Q., Russell, D.H.: On the structure elucidation using ion mobility spectrometry and molecular dynamics. J. Phys. Chem. A **113**, 8221–8234 (2009)
10. Kanu, A.B., Dwivedi, P., Tam, M., Matz, L., Hill, H.H.: Ion mobility-mass spectrometry. J. Mass Spectrom. **43**, 1–22 (2008)
11. Mesleh, M.F., Hunter, J.M., Shvartsburg, A.A., Schatz, G.C., Jarrold, M.F.: Structural information from ion mobility measurements: effects of the long-range potential. J. Phys. Chem. **100**, 16082–16086 (1996)
12. Wyttenbach, T., von Helden, G., Batka, J.J., Carlat, D., Bowers, M.T.: Effect of the long-range potential on ion mobility measurements. J. Am. Soc. Mass Spectrom. **8**, 275–282 (1997)
13. Shvartsburg, A.A., Jarrold, M.F.: An exact hard-spheres scattering model for the mobilities of polyatomic ions. Chem. Phys. Lett. **261**, 86–91 (1996)
14. Shvartsburg, A.A., Liu, B., Jarrold, M.F., Ho, K.-M.: Modeling ionic mobilities by scattering on electronic density isosurfaces: application to silicon cluster anions. J. Chem. Phys. **112**, 4517–4526 (2000)
15. Bleiholder, C., Wyttenbach, T., Bowers, M.T.: A novel projection approximation algorithm for the fast and accurate computation of molecular collision cross-sections (I). Method Int. J. Mass Spectrom. **308**, 1–10 (2011)
16. Clemmer, D.E., Hudgins, R.R., Jarrold, M.F.: Naked protein conformations: cytochrome *c* in the gas phase. J. Am. Chem. Soc. **117**, 10141–10142 (1995)
17. Goldstein, M., Zmiri, L., Segev, E., Wyttenbach, T., Gerber, R.B.: An atomistic structure of ubiquitin +13 relevant in mass spectrometry: theoretical prediction and comparison with experimental cross-sections. Int. J. Mass Spectrom. **367**, 10–15 (2014)
18. Wyttenbach, T., Pierson, N.A., Clemmer, D.E., Bowers, M.T.: Ion mobility analysis of molecular dynamics. Annu. Rev. Phys. Chem. **65**, 175–196 (2014)
19. Wyttenbach, T., Bowers, M.T.: Structural stability from solution to the gas phase: native solution structure of ubiquitin survives analysis in a solvent-free ion mobility-mass spectrometry environment. J. Phys. Chem. B **115**, 12266–12275 (2011)
20. Hall, Z., Robinson, C.V.: Do charge state signatures guarantee protein conformations? J. Am. Soc. Mass Spectrom. **23**, 1161–1168 (2012)
21. Jurneczko, E., Kalapothakis, J., Campuzano, I.D.G., Morris, M., Barran, P.E.: Effects of drift gas on collision cross-sections of a protein standard in linear drift tube and traveling wave ion mobility mass spectrometry. Anal. Chem. **84**, 8524–8531 (2012)
22. Kim, H., Kim, H.I., Johnson, P.V., Beegle, L.W., Beauchamp, J.L., Goddard, W.A., Kanik, I.: Experimental and theoretical investigation into the correlation between mass and ion mobility for choline and other ammonium cations in N_2. Anal. Chem. **80**, 1928–1936 (2008)
23. Shvartsburg, A.A., Schatz, G.C., Jarrold, M.F.: Mobilities of carbon cluster ions: critical importance of the molecular attractive potential. J. Chem. Phys. **108**, 2416 (1998)
24. Dwivedi, P., Wu, C., Matz, L.M., Clowers, B.H., Siems, W.F., Hill, H.H.: Gas-phase chiral separations by ion mobility spectrometry. Anal. Chem. **78**, 8200–8206 (2006)
25. Asbury, G.R., Hill, H.H.: Using different drift gases to change separation factors (α) in ion mobility spectrometry. Anal. Chem. **72**, 580–584 (2000)
26. Warnke, S., Seo, J., Boschmans, J., Sobott, F., Scrivens, J.H., Bleiholder, C., Bowers, M.T., Gewinner, S., Schöllkopf, W., Pagel, K., von Helden, G.: Protomers of benzocaine: solvent and permittivity dependence. J. Am. Chem. Soc. **137**, 4236–4242 (2015)
27. Boschmans, J., Jacobs, S., Williams, J.P., Palmer, M., Richardson, K., Giles, K., Lapthorn, C., Herrebout, W.A., Lemière, F., Sobott, F.: Combining density functional theory (DFT) and collision cross-section (CCS) calculations to analyze the gas-phase behavior of small molecules and their protonation site isomers. Analyst **141**, 4044–4054 (2016)
28. von Helden, G., Hsu, M.T., Gotts, N., Bowers, M.T.: Carbon cluster cations with up to 84 atoms: structures, formation mechanism, and reactivity. J. Phys. Chem. **97**, 8182–8192 (1993)
29. Koeniger, S.L., Merenbloom, S.I., Sevugarajan, S., Clemmer, D.E.: Transfer of structural elements from compact to extended states in unsolvated ubiquitin. J. Am. Chem. Soc. **128**, 11713–11719 (2006)
30. Laszlo, K.J., Munger, E.B., Bush, M.F.: Folding of protein ions in the gas phase after cation to anion proton transfer reactions (CAPTR). J. Am. Chem. Soc. **138**, 9581–9588 (2016)
31. Bleiholder, C., Johnson, N.R., Contreras, S., Wyttenbach, T., Bowers, M.T.: Molecular structures and ion mobility cross-sections: analysis of the effects of He and N_2 buffer gas. Anal. Chem. **87**, 7196–7203 (2015)
32. Liu, F.C., Kirk, S.R., Bleiholder, C.: On the structural denaturation of biological analytes in trapped ion mobility spectrometry-mass spectrometry. Analyst **141**, 3722–3730 (2016)
33. Campuzano, I., Bush, M.F., Robinson, C.V., Beaumont, C., Richardson, K., Kim, H., Kim, H.I.: Structural characterization of drug-like compounds by ion mobility mass spectrometry: comparison of theoretical and experimentally derived nitrogen collision cross-sections. Anal. Chem. **84**, 1026–1033 (2012)
34. Alexeev, Y., Fedorov, D.G., Shvartsburg, A.A.: Effective ion mobility calculations for macromolecules by scattering on electron clouds. J. Phys. Chem. A **118**, 6763–6772 (2014)
35. Bleiholder, C.: A local collision probability approximation for predicting momentum transfer cross-sections. Analyst **140**, 6804–6813 (2015)
36. Mason, E.A., McDaniel, E.W.: Transport Properties of Ions in Gases. Wiley, New York (1988)
37. Jeziorski, B., Moszynski, R., Szalewicz, K.: Perturbation theory approach to intermolecular potential energy surfaces of van der Waals complexes. Chem. Rev. **94**, 1887–1930 (1994)
38. Bleiholder, C., Werz, D.B., Köppel, H., Gleiter, R.: Theoretical investigations on chalcogen−chalcogen interactions: What makes these nonbonded interactions bonding? J. Am. Chem. Soc. **128**, 2666–2674 (2006)
39. Mulliken, R.S.: Electronic population analysis on LCAO-MO molecular wave functions. I. J. Chem. Phys. **23**, 1833 (1955)
40. Finzel, K., Martín Pendás, Á., Francisco, E.: Efficient algorithms for Hirshfeld-I charges. J. Chem. Phys. **143**, 84115 (2015)
41. Reed, A.E., Weinstock, R.B., Weinhold, F.: Natural population analysis. J. Chem. Phys. **83**, 735 (1985)
42. Bader, R.F.: A quantum theory of molecular structure and its applications. Chem. Rev. **91**, 893–928 (1991)
43. Besler, B.H., Merz, K.M.J., Kollman, P.A.: Atomic charges derived from semiempirical methods. J. Comput. Chem. **11**, 431–439 (1990)
44. Chirlian, L.E., Francl, M.M.: Atomic charges derived from electrostatic potentials: A detailed study. J. Comput. Chem. **8**, 894–905 (1987)
45. Lapthorn, C., Pullen, F.S., Chowdhry, B.Z., Wright, P., Perkins, G.L., Heredia, Y.: How useful is molecular modelling in combination with ion

mobility mass spectrometry for "small molecule" ion mobility collision cross-sections? Analyst **140**, 6814–6823 (2015)
46. Politzer, P., Jin, P., Murray, J.S.: Atomic polarizability, volume, and ionization energy. J. Chem. Phys. **117**, 8197 (2002)
47. Wyttenbach, T., Bleiholder, C., Bowers, M.T.: Factors contributing to the collision cross-section of polyatomic ions in the kilodalton to gigadalton range: application to ion mobility measurements. Anal. Chem. **85**, 2191–2199 (2013)
48. Fenn, L.S., Kliman, M., Mahsut, A., Zhao, S.R., McLean, J.A.: Characterizing ion mobility-mass spectrometry conformation space for the analysis of complex biological samples. Anal. Bioanal. Chem. **394**, 235–244 (2009)
49. Paizs, B., Suhai, S.: Fragmentation pathways of protonated peptides. Mass Spectrom. Rev. **24**, 508–548 (2005)
50. Bleiholder, C., Suhai, S., Paizs, B.: Revising the proton affinity scale of the naturally occurring α-amino acids. J. Am. Soc. Mass Spectrom. **17**, 1275–1281 (2006)
51. Bush, M.F., Hall, Z., Giles, K., Hoyes, J., Robinson, C.V., Ruotolo, B.T.: Collision cross-sections of proteins and their complexes: a calibration framework and database for gas-phase structural biology. Anal. Chem. **82**, 9557–9565 (2010)